JOURNAL OF SOLID STATE CHEMISTRY **1**, 310–318 (1970)

Single Crystal Syntheses by the Electrolyses of Molten Titanates, Molybdates and Vanadates

A. F. REID AND J. A. WATTS

Division of Mineral Chemistry, C.S.I.R.O. Melbourne, Australia.

Received October 9, 1969

Electrolyses of alkali titanate and titanate–vanadate melts at temperatures up to 1050°C have produced single crystals of a number of phases of general composition A_xBO_2 where A is an alkali–metal ion and B represents a mixture of Ti^{3+} and Ti^{4+} or of V^{3+} and Ti^{4+}. These phases included hexagonal $Na_{1.3}V_{1.3}Ti_{0.7}O_4$, with lattice parameters $a = 2.92$, $c = 11.20$ Å, the hollandite-types $K_xTi_4O_8$ ($a = 10.20$, $c = 2.99$ Å) and $Cs_xTi_4O_8$ ($a = 10.32$, $c = 2.92$ Å), a potassium layer compound $K_{0.8}V_{0.8}Ti_{1.2}O_4$ ($a = 3.73$, $b = 15.90$, $c = 2.98$ Å) and a cesium layer compound $Cs_xTi_2O_4$ isomorphous with $Rb_xMn_xTi_{2-x}O_4$, with $a = 3.84$, $b = 18.02$, $c = 3.01$ Å.

We have also found a monoclinic sodium titanium oxide of composition near to $NaTiO_2$, with $a = 23.4$, $b = 3.08$, $c = 11.06$ Å, $\beta = 75.25°$, and an octatitanate $K_3Ti_8O_{17}$, with $a = 15.68$, $b = 3.809$, $c = 12.06$ Å and $\beta = 95.0°$. Electrolyses of cesium vanadate and molybdate melts have also produced new phases, including a tetragonal cesium vanadium bronze $Cs_{0.93}V_2O_{5+x}$, $x \approx 0.3$, with $a = 7.72$, $c = 11.73$ Å, and a monoclinic cesium molybdenum bronze $Cs_{0.3}MoO_3$.

The structures of a number of the phases produced have been determined or identified. Most are poor conductors of electricity, but $Cs_xTi_4O_8$ shows highly anisotropic semiconductivity.

Introduction

The electrolysis of molten oxides has been used by a number of workers to prepare compounds in single crystal form. Such compounds have included the tungsten and molybdenum bronzes (*1*), (*2*), and (*3*), MoO_2 (*4*) and (*5*) $Mn_{2-x}Fe_xO_3$ (*6*), $CaTi_2O_4$ (*7*) and (*8*), CaV_2O_4(*9*), $Co_{1+x}V_{2-x}O_4$(*10*), and the borate compounds of typical composition $Mg_4B_2V_2O_{10}$ (*11*). When the crystals are deposited at the cathode, as is usual in electrolytic preparations, they contain at least one of the constituent metals in an oxidation state lower than that normally exhibited.

Our recent work (*12*), (*13*), and (*14*) on ternary alkali titanate systems A_2O–M_2O_3–TiO_2 in which M is any of a number of metal ions with a normal valency of +3 has led us to expect a variety of such compounds in which M is Ti^{3+} or V^{3+}. Several compounds with $M = Ti^{3+}$ have previously been prepared by solid state reactions (*15*) and (*16*) or by hydrogen reduction (*17*) and (*18*). In the present work, we have by the electrolysis of molten alkali titanate or titanate–vanadate compositions at temperatures up to 1050°C, produced in single crystal form compounds with $M = Ti^{3+}$ or V^{3+}.

An unexpected discovery was the stabilization of particular structures by the addition of small quantities of other oxides to titanate melts. For several systems we have also found, as was demonstrated by Wold in his work on molybdenum bronze (*3*), that the compound formed depends on both the composition and the temperature of the melt. In addition to the titanate systems, we have electrolysed cesium molybdate and vanadate melts, and in the present paper we wish to report on our experimental procedures, the synthesis in single crystal form of new compounds of known structure, and the synthesis of several new compounds whose structures will be reported subsequently.

Experimental

Preparation of Starting Materials and Melts

Where possible the melting points of desired compositions were obtained from published phase diagrams. The end member compounds of the composition ranges to be studied were then synthesised in powder form by solid state reaction 30–50° below their melting points or incongruent decomposition temperatures. Compounds thus prepared included Na_2TiO_3, $K_2Ti_2O_5$, $Cs_2Ti_2O_5$, $CsVO_3$ and Cs_2MoO_4 Starting materials included $Na_2C_2O_4$, K_2CO_3,

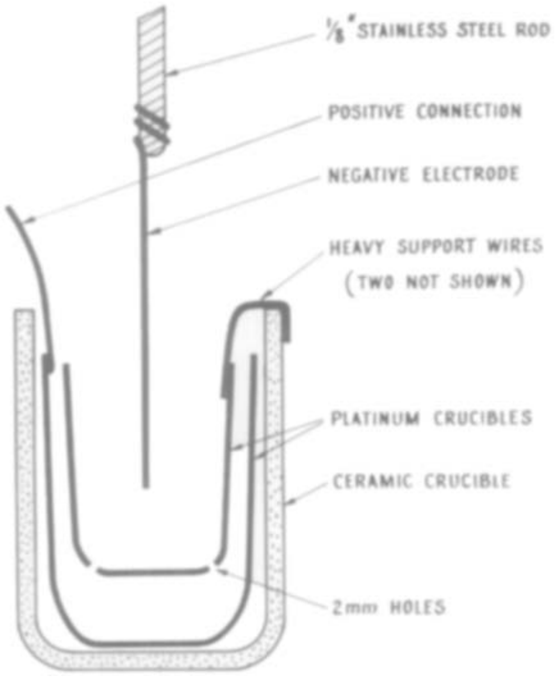

FIG. 1. Electolysis crucible assembly.

$CsNO_3$, NH_4VO_3, and the oxides TiO_2 (anatase form) and MoO_3.

To obtain a melt of given composition, appropriate quantities of the end member and the component oxide were finely mixed, packed into the electrolysis crucible and melted into place. As it was usually necessary to add more than one charge of powdered material, the premelting procedure was carried out in a muffle furnace.

Electrolysis Procedure

The cell consisted of two standard platinum crucibles mounted concentrically, the outer being supported in an alumina crucible, and the inner by means of three arms of heavy platinum wire welded to its rim and bent back over the edge of the alumina crucible (Fig. 1). The inner crucible was penetrated by six holes, 2 mm in diameter, drilled at the bottom edge of its wall. These holes provided a suitable conduction path from the outer crucible, which acted as the anode, to a 1-mm platinum wire (cathode) suspended in the melt in the inner crucible. The wire was held on the end of an $\frac{1}{8}$-in. stainless steel rod which could be raised or lowered through a sliding seal on the head of the vessel (Fig. 2). The cell arrangement, which had the considerable advantage of being constructed from standard crucibles, was easy to repair or replace.

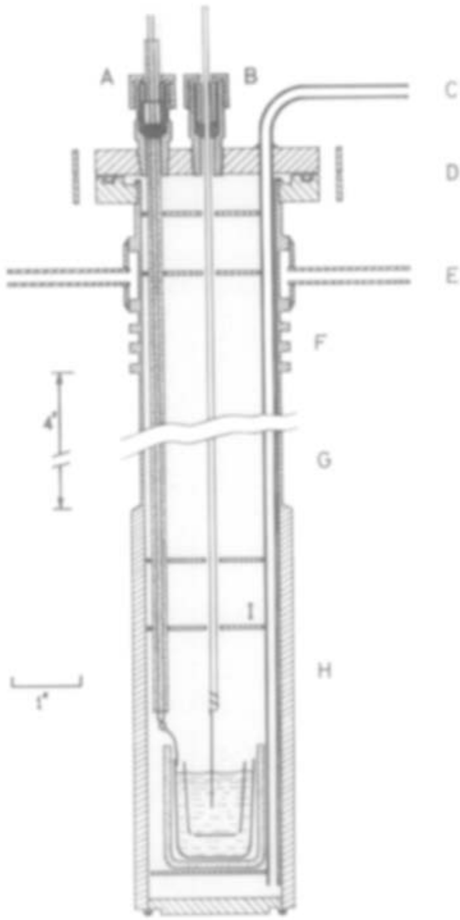

FIG. 2. Inconel electrolysis vessel. Ceramic is stippled, Teflon is crosshatched. *A*—Seal for positive electrical connection (Conax Co.). A similar seal, not shown, carries a thermocouple. *B*—Sliding seal for $\frac{1}{8}$-in. stainless steel rod connecting to negative electrode. *C*—Argon inlet. Outlet, not shown, has no extension into the vessel. *D*—Stainless-steel flanges. Bolts not shown. *E*—Water connection. *F*—Cooling fins. *G*—Thin-walled section, 0.050-in. *H*—Heavy wall uniform temperature section. *I*—Radiation shields. Support rods, of $\frac{1}{8}$-in. stainless steel, are not shown.

The crucible assembly was held in a welded vessel whose body and base were constructed of Inconel, and which was fitted with stainless steel flanges sealed with a Viton O-ring, Fig. 2. Overheating of the seal was prevented by passage of cooling water through an annular space just below the flange. The gap between the vessel and the tube furnace was, in its upper 1 or 2 in., tightly packed with mullite wool (Morganite Co.). This severed both as insulation and as a diffusion barrier to contain a protective atmosphere of argon around the vessel.

Radiation shields and the support plate for the

TABLE I

SINGLE CRYSTAL PRODUCTS FROM MOLTEN OXIDE ELECTROLYSIS

Melt composition (mole %)	Run no.	T °C	I_a mA	Time hours	Product (crystal sizes in mm and *inferred* compositions in parentheses)	Structure type	Unit cell dimensions, Å
Na_2TiO_3 (76), TiO_2 (18), Al_2O_3 (6)	1	1030	60	3.5	Blue-black needles 2 × 1 × 1, approx. $NaTiO_{2+x}$, $0 < x < 0.5$, plus 1 wt% Al_2O_3	New monoclinic phase	a = 23.4, b = 3.08, c = 11.06, β = 75.25°
Na_2TiO_3 (76), TiO_2 (18), Al_2O_3 (6)	2	1030	60	20	Blue-black prisms 10 × 2 × 2	As in Run 1	As in Run 1
Na_2TiO_3 (67.5), TiO_2 (32.5)	3	1020	80	16	Small black crystals	As in Run 1	As in Run 1
Na_2TiO_3 (73), $NaVO_3$ (27)	4	985	100	16	Dark brown plates 5 × 5 × 1, approx. $Na_{1.3}V_{1.3}Ti_{0.7}O_4$	$Na_{1.33}Ni_{0.67}Ti_{1.33}O_4$ (*22*)	a = 2.94 c = 11·20
$K_2Ti_2O_5$ (100)	5	1020	100	16	Mass of blue-black prisms 8 × 1 × 1, ($K_xTi_4O_8$, $x \leqslant 1$)	Potassium hollandite (*29*)	a = 10.20 c = 2·99
$K_2Ti_2O_5$ (93), Al_2O_3 (7)	6	1050	100	16	Same as Run 6	Potassium hollandite (*29*)	a = 10.15, c = 2.99
$K_2Ti_2O_5$ (98.5), Nb_2O_5 (1.5)	7	1010	100	16	Small needle-like crystals ($K_3Ti_8O_{17}$)	Potassium octatitanate (*31*)	a = 15.68, b = 3.809 c = 12.06, β = 95.0°
$K_2Ti_2O_5$ (98.5), Nb_2O_5 (1.5)	8	980	60	16	Large black prisms	Potassium hollandite (*29*)	a = 10.20, c = 2.99
$K_2Ti_2O_5$ (73), KVO_3 (27)	9	990	100	16	Dark brown plates 2 × 3 × 0.2, approx. $K_{0.7}V_{0.7}Ti_{1.3}O_4$	$K_{0.8}Mg_{0.4}Ti_{1.6}O_4$ (*14*)	a = 3.73, b = 15.90, c = 2.98
$Cs_2Ti_2O_5$ (82), TiO_2 (18)	10	925	100	16	Dark bronze lustrous prisms 4 × 1 × 1, ($Cs_xTi_4O_8 \leqslant 1$)	Cesium hollandite (*18*)	a = 10.32 c = 2.92
$Cs_2Ti_2O_5$ (82), TiO_2 (18)	11	905	100	16	Black plates 1 × 1 × 0.1, ($Cs_{0.7}Ti_2O_4$)	Rubidium manganese titanate (*13*)	As in Run 12
Cs_2O (43), TiO_2 (57)	12	885	200	16	Black hexagonal plates 2 × 2 × 0.5, ($Cs_{0.7}Ti_2O_4$)	Rubidium manganese titanate (*13*)	a = 3.84, b = 18.02, c = 3.01
Cs_2MoO_4 (50), MoO_3 (50)	13	525	100	20	Large black crystals of MoO_2	MoO_2 (*5*)	a = 5.61, b = 4.86, c = 5.63, β = 121°
Cs_2MoO_4 (30), MoO_3 (70)	14	530	150	22	Small copper coloured crystals, (Cs_xMoO_3)	New monoclinic structure, $Cs_{1/3}$ MoO_3 (*42*)	a = 6.4, b = 7.7, c = 8.14, β = 96°
Cs_2O (44), V_2O_5 (56)	15	585	80	16	Black plates 3 × 3 × 0.5	New orthorhombic phase	a = 6.65, b = 7.70, c = 9.62
Cs_2O (37), V_2O_5 (63)	16	540	80	20	Dark brown prisms 5 × 1 × 1, approx. $Cs_{0.94}V_2O_{5.3}$	New tetragonal phase	a = 7.72 c = 11.73

[a] Cathode area approximately 0.25 cm².

crucible assembly were suspended on three $\frac{1}{8}$-in. stainless steel rods threaded into the top flange, which also carried gas-tight glands for electrical connections and thermocouple leads, and an argon inlet tube. In a typical run the vessel was flushed with argon and brought up to operating temperature with the centre electrode raised. The electrode was then lowered 8–10 mm below the melt surface, and a controlled current of 60–200 mA passed for a period of 3–40 h. At the conclusion of electrolysis the central electrode and its attached crystals were lifted clear of the melt. The vessel was then allowed to cool to room temperature before removal of the top flange with the crucible assembly suspended from it.

Recovery and Characterization of Products

In most runs, the crystalline product was attached to the central wire and could be broken from it. If the products were stable to dilute acids any solidified melt could be dissolved away, and if not, crystals were hand picked from the lightly crushed mixtures. A Guinier camera was used to obtain X-ray powder patterns for lattice parameter determinations, except when the products exhibited strong preferred orientation, in which case a Debye–Scherrer camera was used. Single crystal rotation and Weissenberg photographs were used both as an aid to the indexing of powder patterns and for identification purposes. Several compounds were obtained in sufficient yield for quantitative analysis, Table I. These analyses were performed by the Analytical Group of the Division of Mineral Chemistry.

Results

The experimental conditions under which the most significant results were obtained are summarized in Table I. The nature of the products and the behaviour of the various systems are discussed in more detail in the following sections.

Na_2TiO_3–TiO_2

Only a few compounds containing sodium and Ti^{3+} are so far known. These include $NaTiO_2$ (*15*), of formal composition $Na_2O \cdot Ti_2O_3$ and Na_xTiO_2, $0.20 < x \leqslant 0.25$ (*17*), of formal limiting composition $Na_2O \cdot Ti_2O_3 \cdot 6TiO_2$. $NaTiO_2$ and Na_xTiO_2 are, respectively, isomorphous with α-$NaFeO_2$ (*19*) and $NaFeTi_3O_8$ (*20*), and the two sets of compounds are members of pseudobinary systems $NaTi^{3+}O_2$–TiO_2 and $NaFeO_2$–TiO_2. In the latter system the compounds $NaFeTiO_4$ (*12*) and $Na_xFe_xTi_{2-x}O_4$, $0.75 < x < 0.90$ (*21*), are also known, although their Ti^{3+} isotypes have not as yet been prepared.

It was expected that the electrolysis of Na_2TiO_3–TiO_2 melts near the eutectic at 27 mole% TiO_2, Fig. 3, would lead to one of the known Ti^{3+} compounds, or possibly to one of the other structures known in the Fe^{3+} system. Instead, metallic sodium was evaporated from the melts. The free energy of the reaction,

$$Na_2O + Ti_2O_3 \rightleftharpoons 2Na + 2TiO_2,$$

passes from slightly positive to slightly negative values as the temperature rises through 800–900°C (*15*), and liberation of sodium metal has been observed to occur when either of the solids $NaTiO_2$ (*15*) or $Na_{0.25}TiO_2$ (*16*) is heated above 800°C. In melts containing high concentrations of sodium, it is therefore likely that sodium metal is liberated at the cathode in preference to Ti^{3+}. However, electrolysis of a melt in inadvertent contact with an alumina crucible gave a mass of large blue-black crystals. These had a sodium-titanium ratio close to unity, but also contained 0.5–1% by weight of Al_2O_3. They gave a strongly alkaline reaction when treated with water. The compound proved to have a new monoclinic structure characterized by a 3 Å *b* axis (an octahedral edge length) and large *a* and *c* axes of 23.4 and 11.06 Å, respectively. A description of this structure will be given elsewhere. Addition of approximately 6 mole% of Al_2O_3 to a 0.81 Na_2TiO_3–0.19 TiO_2 mixture gave a melt which on electrolysis yielded crystals of the new phase up to 10 × 2 × 2 mm in size, Runs 1 and 2, Table I. The structure is possibly stabilized by Al^{3+} ions randomly substituted for Ti^{3+}, but it is equally likely that the presence of alumina in the melt lowered the sodium activity and allowed Ti^{3+} to be produced. A moderate yield of the new phase was indeed obtained in the absence of alumina when the titania content of the melt was increased to 33 mole% (Run 3).

Na_2TiO_3–$NaVO_3$

The preparation of a new sodium titanium oxide in the presence of alumina suggested that other oxides could also act to allow such structures to form. In addition, the existence of a large number of Na_2O–A_2O_3–TiO_2 phases made it appear likely that Na_2O–V_2O_3–TiO_2 compounds could be synthesized, and the electrolytic reduction of V^{5+} to V^{3+} could well provide the necessary mechanism for the formation of such compounds in single crystal form.

The system Na_2TiO_3–$NaVO_3$ was chosen as having a suitable eutectic near 20 mole% $NaVO_3$, Fig. 3, but electrolysis at this composition failed to give a reduced species. However, at 27 mole%

$NaVO_3$ (Run 4) large brown tabular crystals were formed which exhibited a pronounced mica-like cleavage. They did not react with dilute acid, and were easily separated from the bulk of the melt by dissolution of the latter in 2*N* HCl. Single crystal X-ray photographs showed them to be hexagonal with $a = 2.94$ Å and $c = 11.20$ Å. Debye–Scherrer photographs confirmed these lattice parameters and showed the compound to have reflection intensities almost identical with those of $Na_{1.33}Ni_{0.67}Ti_{1.33}O_4$, a recently discovered (*22*) hexagonal layer compound with $a = 3.05$, $c = 11.20$ Å.

Chemical analysis showed that it had a composition very close to $Na_{1.3}V_{1.3}Ti_{0.7}O_4$, namely $Na_{2-x}(A + Ti)_2O_4$, $x \approx 0.7$, the general formula characterizing the sodium nickel titanate and its cobalt isomorph (*22*). The structure is similar to that of α-$NaFeO_2$, but with the sodium layers only partially occupied. In addition the correspondence between the layers of metal–oxygen octahedra is altered, so that the structure is truly hexagonal rather than rhombohedral and contains only two such layers per unit cell instead of three. The *c* axis is thus 11 Å ($\frac{2}{3}$ of 16 Å) rather than 16 Å as in α-$NaFeO_2$. A similar structure has been reported for $KPb_{0.33}Ti_{0.67}O_2$ by Fouassier and Hagenmuller (*41*).

The valencies of vanadium and titanium in the new compound have not been determined by chemical methods, but as the structure requires a mixture of 3+ and 4+ ions in the ratio 1.3–0.7, and since the reaction

$$2VO_2 + Ti_2O_3 \xrightarrow{1000°C} V_2O_3 + 2TiO_2$$

is exothermic by −20 kcal per mole of Ti_2O_3 (*23*), it is expected that even if Ti^{3+} ions are formed in the initial electrode processes, the final structure will contain only V^{3+} and Ti^{4+}.

Systems Based on $K_2Ti_2O_5$

Hollandite (*27*) isotypes of limiting composition $KAlTi_3O_8$ and $KFeTi_3O_8$ have been synthesized (*28*) and Wadsley and Andersson (*29*) have reported that one of the products of hydrogen reduction of $K_2Ti_2O_5$ is an intensely blue-black compound with this same structure and thus of formal composition $K_xTi_x^{3+}Ti_{4-x}^{4+}O_8$, $x \leq 1$. Electrolysis of $K_2Ti_2O_5$, which melts congruently at 942°C, could also be expected to give $K_xTi_4O_8$ of hollandite form, and did indeed do so, Run 5. The compound was formed as large masses of black crystals up to 8 × 1 × 1 mm in size. It was inert to dilute acids, and was readily separated from the potassium titanate residue.

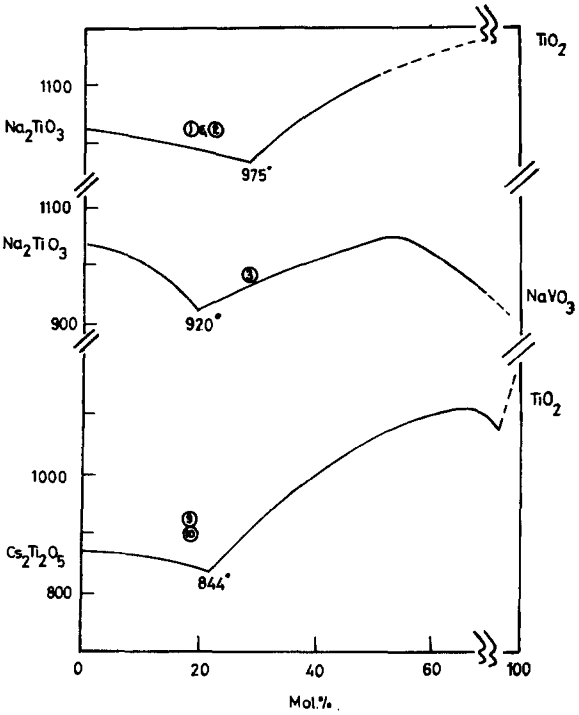

FIG. 3. Systems Na_2TiO_3–TiO_2 (*24*), Runs 1, 2 and 3; Na_2TiO_3–$NaVO_3$ (*25*), Run 4; K_2TiO_3–KVO_3 (*25*); $Cs_2Ti_2O_5$–TiO_2 (*26*), Runs 10 and 11.

The formation of new phases by electrolysis of sodium titanate melts containing Al_2O_3 or V_2O_5 suggested that similar effects might operate in the potassium titanate systems. In addition, Nb^{5+} is known to substitute randomly for Ti^{4+} in compounds such as $KTiNbO_5$ and KTi_3NbO_9 (*30*), and it was considered that the presence of Nb^{5+} might stabilize yet other structures. We consequently examined $K_2Ti_2O_5$ melts to which Al_2O_3, Fe_2O_3, KVO_3 and Nb_2O_5 had been added.

$K_2Ti_2O_5$–Al_2O_3

Approximately 7 mole % of Al_2O_3 was found to be soluble in $K_2Ti_2O_5$ melts at 1000°C. An electrolysis of such a melt at 1050°C (Run 6) gave a potassium hollandite phase with parameters much closer to those of $K_xTi_4O_8$ than those of $KAlTi_3O_8$ [for which $a = 10.04$ Å, $c = 2.94$ Å (*28*)], indicating that only small quantities of Al^{3+} had entered the structure.

$K_2Ti_2O_5$–Fe_2O_3

Electrolysis of a $K_2Ti_2O_5$ melt containing 5 mole % of Fe_2O_3 led to the formation of metallic crystals of a highly reactive magnetic iron–platinum alloy.

Reduction conditions during electrolysis were evidently too severe for the Fe^{2+} or Fe^{3+} oxidation states to be retained.

$K_2Ti_2O_5$–Nb_2O_5

Electrolysis at 1010°C of a melt containing 1.5 mole% of Nb_2O_5 (Run 7) gave a massive fibrous grey deposit containing black needle-like crystals. Single crystal photographs showed that this was a new phase, apparently related to the alkali–metal hexatitanates. Subsequent refinement of the structure (*31*) showed it to be an octatitanate $K_3Ti_8O_{17}$ of formal composition $K_3{}^{+}Ti^{3+}Ti_7^{4+}O_{17}$. The stabilization of this structure by niobium is most probably due to a small amount of Nb^{5+} substituting for Ti^{4+} as in the potassium niobates (*30*), with over-all charge compensation being obtained by the simultaneous substitution of additional Ti^{3+} for Ti^{4+}. For the pure oxides the stable pair is Ti_2O_3/Nb_2O_5 rather than TiO_2/NbO_2, and this combination is likely to persist in a ternary or quaternary compound. We were unable to confirm chemically the presence of niobium in the phase, as it proved impossible to dissolve the last traces of melt without destroying the crystals. A further run at 990°C gave the same octatitanate product, but at 980°C the major product was potassium hollandite, Run 8.

$K_2Ti_2O_5$–KVO_3

The pseudobinary system K_2TiO_3–KVO_3 (*25*) contains a low melting region in the composition range 0–25 mole% of KVO_3, and we found that the $K_2Ti_2O_5$–KVO_3 system showed somewhat similar behaviour. No product was obtained by electrolysis at 1000°C of melts containing 11.5–20 mole% KVO_3, but at 27 mole% KVO_3 and 73 mole% $K_2Ti_2O_5$, relatively large dark brown "platey" crystals were formed at 880°C, Run 9. These crystals gave Weissenberg patterns quite similar to those of $Rb_xMn_xTi_{2-x}O_4$ (*13*), and indicative of considerable disorder in the crystal. However, careful examination of the films showed them to be characterized by the space group Pnma rather than Cmcm.

The powder diffraction pattern obtained from ground up crystals corresponded to a unit cell with dimensions $a = 3.73$, $b = 15.90$, and $c = 2.98$ Å, close to those for $Rb_xMn_xTi_{2-x}O_4$, but with the different reflections required by the differences in space group symmetries. Solid state synthesis of various nonreduced phases of appropriate stoichiometry showed that $K_{0.75}Sc_{0.75}Ti_{1.25}O_4$ and $K_{0.8}Mg_{0.4}Ti_{1.6}O_4$ for example were strictly isostructural with the new vanadate phase, which thus has a composition near to $K_{0.8}V_{0.8}Ti_{1.2}O_4$. A single crystal structure determination for $K_{0.8}Mg_{0.4}Ti_{1.6}O_4$ showed that the structure consists of double layers of edge-shared metal oxygen octahedra separated by layers of potassium ions. The structure, which is fully described in a separate paper (*14*), resembles that of $Rb_xMn_xTi_{2-x}O_4$, with a unit cell of similar size. However, the correspondence between the layers is altered, and the local coordination for the alkali ion is different.

System Cs_2O–TiO_2

Addition of 22 mole% of TiO_2 to the congruently melting compount $Cs_2Ti_2O_5$ (*26*) produces a eutectic melting at 844°C, Fig. 3; the composition $Cs_2O \cdot TiO_2$ melts at 698°C (32), but does not correspond to a compound. It was considered, by analogy with the $RbMnO_2$–TiO_2 system (*13*) (which typifies a number of $RbBO_2$–TiO_2 and $CsBO_2$–TiO_2 systems in which B is a 3+ ion) that electrolysis of cesium titanate melts would yield one or more of the Ti^{3+} compounds $CsTiO_2$, $Cs_xTi^{3+}Ti_{2-x}^{4+}O_4$, $x \approx 0.7$, (isomorphous with $Rb_xMn_xTi_{2-x}O_4$) or cesium hollandite $Cs_xTi^{3+}Ti_{4-x}^{4+}O_8$, $x \leqslant 1$, (*18*). The two compounds with higher titanium content were indeed found; high titania concentrations and higher temperatures (Run 10) favoured the formation of the hollandite, while lower temperatures (Run 11) and higher cesium contents (Run 12) allowed the formation of the $Cs_xTi_2O_4$ layer compound isomorphous with $Rb_xMn_xTi_{2-x}O_4$.

At the composition $Cs_2O \cdot TiO_2$ the compound $CsTiO_2$ was not formed, instead, metallic cesium was evaporated from the melt. This behaviour is analogous to that observed in the Na_2O–TiO_2 system. However, addition of a modest amount of TiO_2 to $Cs_2O \cdot TiO_2$ melts allowed the formation of quite large hexagonally shaped tablets of the orthorhombic layer compound $Cs_xTi_2O_4$, Run 12.

Despite its higher Ti^{3+} content the layer compound was effectively nonconducting, with $\rho < 10^{-5}\ \Omega^{-1}$ cm However, the hollandite compound, $Cs_xTi_4O_8$, $x \leqslant 1$, which formed as large, dark, bronze-coloured crystals, showed strong anisotropic semiconductivity, with $\rho_{20C} = 0.42\ \Omega^{-1}$ cm along the c axis.

System Cs_2O–MoO_3

Potassium molybdenum bronzes were prepared by Wold et al. (3) by electrolysis of K_2MoO_4–MoO_3 melts in liquidus regions adjacent in composition to and lower in temperature than the congruent melting points defined in the phase diagram. At temperatures above such congruent melting points MoO_2 was formed (*3*), (*4*) and (*5*). The Cs_2O–MoO_3 system (*33*) is very similar to the K_2O–MoO_3

system (*34*), and it was considered that a comparable experimental approach could produce cesium molybdenum bronzes.

Electrolysis at 525°C of a 1:1 $CsMoO_4$–MoO_3 melt, a composition region adjacent to that of $Cs_2Mo_3O_{10}$ which melts at 550°C, produced only crystals of monoclinic MoO_2, with lattice parameters essentially the same as those reported by Brandt et al. (*5*), Run 13. However, electrolysis at 530°C of a 30 mole% Cs_2MoO_4–70 mole% MoO_3 melt (Run 14) gave small but well-developed copper coloured crystals of a monoclinic cesium molybdenum bronze. These were insoluble in dilute acid, and easily separated from the melt by dissolution of the latter. The structure of this new phase is related to those of the potassium molybdenum bronzes, and corresponds to the limiting composition $Cs_{1/3}MoO_3$. This structure will be described in detail elsewhere (*42*).

Electrolysis at 538°C of a melt containing Cs_2MoO_4 and MoO_3 in the molar ratio 24:76 gave a large deposit of bronze-coloured crystals which proved to be MoO_2 with a notably different appearance from that produced in Run 13, but with the same lattice parameters.

System Cs_2O–V_2O_5

The existence of the well-characterized lithium, sodium, and potassium vanadium bronzes, recently reviewed by Banks and Wold (*2*), suggested that cesium may also form bronzes with vanadium oxides, or possibly new phases containing vanadium entirely as V^{3+} or as V^{4+} ions.

Following the procedure adopted for molybdenum bronze syntheses, we electrolysed Cs_2O–V_2O_5 melts (*35*) at compositions adjacent to the liquidus boundaries of the congruently melting compounds $CsVO_3$ and CsV_3O_8, Fig. 4. At 44 mole% Cs_2O and 56 mole% V_2O_5, electrolysis at 585°C gave black plate-like crystals of a new orthorhombic phase Run 15. Electrolysis of a melt containing 37 mole% Cs_2O and 63 mole% V_2O_5, Run 16, gave a large mass of dark coloured columnar crystals which proved to have tetragonal symmetry. Analysis for Cs, V^{5+} and total vanadium showed the Cs:V ratio to be close to 0.47:1 and that close to 80% of the vanadium was present as V^{5+}. When the compound was dissolved in dilute hydrochloric acid in the absence of air, a blue solution was formed which exhibited strong optical absorption at 5900 cm^{-1} and 13,300 cm^{-1}, with a shoulder at 16,500 cm^{-1}. These values are characteristic of V^{4+} (*36*) and not of V^{3+}. Thus the composition can be expressed as being near to $Cs_{0.94}V_2O_{5.3}$. However, the exact stoichiometry, and particularly that of the structural framework if Cs sites are only partly occupied, must be determined from the crystal structure. A study of the structure is in progress, and will be reported in due course.

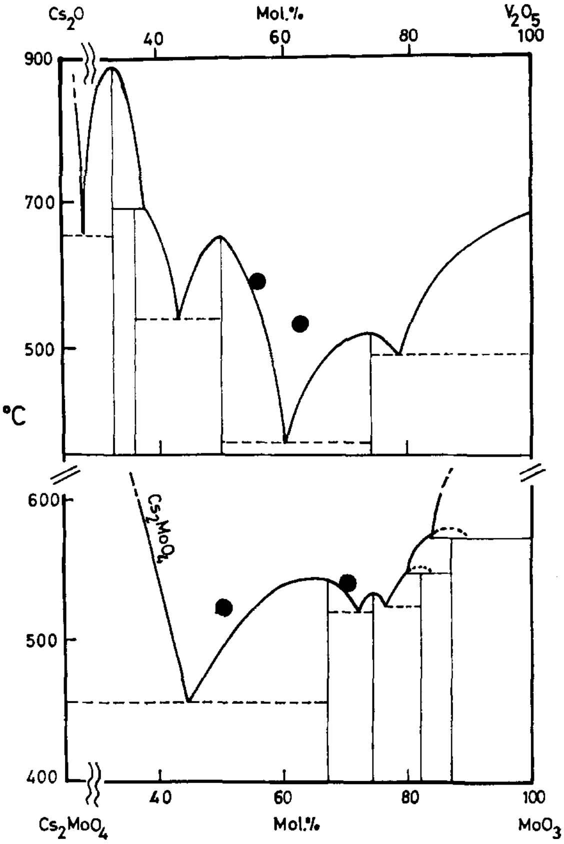

FIG. 4. Systems Cs_2MoO_4–MoO_3 (*33*), Runs 13 and 14; Cs_2O–V_2O_5 (*35*), Runs 15 and 16.

Discussion

The structures which we have identified for the alkali-metal compounds produced in the present work are all based on three-dimensional frameworks of metal–oxygen polyhedra which enclose sites for alkali-metal ions. In general, the extent to which these sites are occupied is fully charge compensated either by a reduction in valency of metal ions in the host framework, or by their replacement by other ions of lower valency. However, potassium octatitanate, with a formal composition $K_3Ti^{3+}Ti_7^{4+}O_{17}$, has only one third of the potassium ions charge compensated in this manner, and the tetragonal cesium vanadium oxide phase, Run 16, Table 1, contains considerably more Cs^+ than V^{4+}.

Except for $K_3Ti_8O_{17}$, which is structurally related (*31*) to the binary titanate $Na_2Ti_6O_{13}$ (*37*) all of the alkali-metal titanate compounds lie on the pseudobinary tie lines AMO_2–TiO_2 of the ternary systems A_2O–M_2O_3–TiO_2, and can thus be described by the general formula A_xBO_2, $0.25 < x < 1$. For the present compounds M is Ti^{3+} or V^{3+}, but each has a number of isotypes in which M is a variety of 3+ ions or equimolar mixtures of 2+ and 4+ ions. Thus, $Na_{1.3}V^{3+}_{0.7}Ti^{4+}_{1.3}O_4$ is isostructural with $Na_{1.33}Ni_{0.67}Ti_{1.33}O_4$, (*22*); $K_{0.8}V^{3+}_{0.8}Ti_{1.2}O_4$ is isostructural with $K_{0.8}Mg_{0.4}Ti_{1.6}O_4$ (*14*); $Cs_xTi_2O_4$ is isostructural with $Rb_xMn_xTi_{2-x}O_4$ (*13*); and the hollandites $K_xTi_4O_8$ and $Cs_xTi_4O_8$ are isostructural with hollandites of typical composition $Cs_{0.7}Fe_{0.7}Ti_{3.3}O_8$ (*38*).

In the formation of these compounds, the principal function of the electrolysis process is to provide ions of lower charge than normally exist in the oxide melts. However, reduction mechanisms do not necessarily involve liberation of individual reduced metal ions. It is quite probable that polyanions existing in the oxide melts have only one of their component metal ions reduced in valency, thus providing precursor fragments which can combine with alkali-metal ions to form crystalline solids. The second step need not be instantaneous, and the formation of crystals throughout the cathode region of titanate and other melts may well be due to diffusion of reduced polyanionic fragments away from the cathode. Such mechanisms are obviously difficult to determine, and so far little or nothing is known of the electrolysis processes leading to single crystal formation.

Electrical conductivity and other properties of individual compounds are determined largely by the structure of the host framework and the metal ions which it contains. While we have not made extensive conductivity studies on the compounds reported, dc potential probe measurements showed that the compounds containing V^{3+} had conductivities lower than 10^{-5} Ω^{-1} cm, as did $Cs_xTi_2O_4$ and the tetragonal cesium vanadium phase, Run 16. The most interesting compound examined was the cesium titanium bronze $Cs_xTi_4O_8$. It showed high semiconductivity along the c axis, with $\rho = 0.42$ Ω^{-1} cm at 20°C and $\rho = 0.098$ Ω cm^{-1} at 80°C, with linear dependence of $\log \rho$ on $1/T$. Across the c axis however the conductivity was less than 10^{-5} Ω^{-1} cm. The direction of ready semiconductivity corresponds to the 2.94 Å distance in which the structure repeats by the edge-sharing of metal–oxygen octahedra already joined in pairs by edge-sharing (*27*) and (*38*). The strings of edge-shared double blocks so formed, extending infinitely in the c axis direction, are "corner joined" in the a–b plane to form tunnels which accommodate the Cs^+ ions. It is in this corner-joining direction that conductivity is extremely low.

Conduction along the directions of continued edge-sharing is probably due to extended Ti(3*d*)–O(2*p*)–Ti(3*d*) orbital overlap. A comparison can be made with the nonconducting compound $CaFe_2O_4$, which contains similar strings of edge-shared double blocks (*12*), corner joined to form tunnels for Ca^{2+}. $CaFe_2O_4$ exhibits very strong ferromagnetic, or above 180°K, antiferromagnetic interactions along the edge-sharing repeat direction while interactions between corner-joined blocks are very weak (*38*), (*39*) and (*40*). The super-exchange coupling (metal–oxygen–metal orbital overlap) which allows these interactions in $CaFe_2O_4$ could well allow actual transfer of electrons in $Cs_xTi_4O_8$, although conductivity via direct 3*d* overlap is not necessarily precluded. A study of the electrical and magnetic properties of $Cs_xTi_4O_8$ should be most informative.

Acknowledgements

We are greatly indebted to Mr. E. S. Pilkington of the Division of Mineral Chemistry Analytical Group, who performed most of the analyses reported in this paper, and to the late Dr. A. D. Wadsley who first suggested the electrolysis of sodium titanate melts to us.

References

1. L. D. Ellerbeck, H. R. Shanks, P. H. Sidles, and G. C. Danielson, *J. Chem. Phys.* **35**, 298 (1961).
2. E. Banks and A. Wold, "Oxide Bronzes," *in* "Preparative Inorganic Reactions," (W. L. Jolly, Ed.), Vol. 4, Interscience, New York, 1967.
3. A. Wold, W. Kunnmann, R. J. Arnott, and A. Feretti, *Inorg. Chem.* **3**, 545 (1964).
4. M. Guichard, *Compt. Rend.* **129**, 724 (1899).
5. B. G. Brandt and A. C. Skapski, *Acta. Chem. Scand.* **21**, 661 (1967).
6. E. Banks and E. Kostiner, *J. Appl. Phys.* **37**, 1423 (1966).
7. E. F. Bertaut and P. Blum, *Acta Cryst.* **9**, 121 (1956).
8. N. F. H. Bright, J. F. Rowland and J. G. Wurm, *Can. J. Chem.* **36**, 492 (1958).
9. E. F. Bertaut, P. Blum and P. Magnano, *Compt. Rend.* **241**, 757 (1955).
10. D. B. Rogers and A. Ferreti, *J. Phys. Chem. Solids* **27**, 1445 (1968).
11. P. Blum and H. Bozon, *Compt. Rend.* **238**, 811 (1954).
12. A. F. Reid, A. D. Wadsley and M. J. Sienko, *Inorg. Chem.* **7**, 112 (1968).
13. A. F. Reid, W. G. Mumme and A. D. Wadsley, *Acta Cryst.* **24A**, 1228 (1968).
14. W. G. Mumme, A. F. Reid and J. A. Watts (to be published).
15. P. Hagenmuller, A. Lecerf and M. Onillon, *Compt. Rend.* **255**, 928 (1962).
16. A. F. Reid and M. J. Sienko, *Inorg. Chem.* **6**, 321 (1967).

17. S. Andersson and A. D. Wadsley, *Acta Cryst.* **15**, 201 (1962).
18. M. Lundberg and S. Andersson, *Acta Chem. Scand.* **18**, 817 (1964).
19. S. Goldstaub, *Compt. Rend.* **196**, 280 (1933).
20. G. Bayer and W. Hoffman, *Z. Krist.* **121**, 9 (1965).
21. W. G. Mumme and A. F. Reid, *Acta Cryst.* **B24**, 625 (1968).
22. W. G. Mumme and A. F. Reid (to be published).
23. O. Kubaschewski, E. Ll. Evans and C. G. Alcock, "Metallurgical Thermochemistry," 4th ed., Pergamon Press, London, England, 1967.
24. I. N. Belyaev and N. P. Sigida, *Zhur. Neorg. Khim.* **3**, 425 (1958).
25. M. L. Sholokhovich and G. V. Barkova, *Zhur. Obshchei Khim.* **26**, 1270 (1956).
26. O. Schmitz-DuMont and H. Rickhard, *Monatsh. Chem.* **90**, 135 (1959).
27. A. Byström and A. M. Byström, *Acta Cryst.* **3**, 146 (1950).
28. G. Bayer and W. Hoffman, *Amer. Mineralogist* **51**, 511 (1966).
29. A. D. Wadsley and S. Andersson, *Nature* **192**, 551 (1961).
30. A. D. Wadsley, *Acta Cryst.* **17**, 623 (1964).
31. J. A. Watts, *J. Solid State Chem.* **1**, Nos. 3–4, 319–325 (1969).
32. "Gmelins Handbuch der Anorganischen Chemie," **41**, 413. Verlag Chemie Gmbh, Weinheim, Germany, 1951.
33. V. Spitsyn and I. M. Kuleshov, *Zhur. Obshchei Khim.* **21**, 1371 (1951).
34. V. Spitsyn and I. M. Kuleshov, *Zhur. Obshchei Khim.* **21**, 1367 (1951).
35. "Gmelins Handbuch der Anorganischen Chemie," **48B2**, 493. Verlag Chemie Gmbh, Weinheim, 1967.
36. C. J. Ballhausen, "Introduction to Ligand Field Theory," p. 229, McGraw-Hill Book Co., New York, 1962.
37. S. Andersson and A. D. Wadsley, *Acta Cryst.* **15**, 194 (1962).
38. J. Birchall, N. N. Greenwood, and A. F. Reid, *J. Chem. Soc.* 1969 (in press).
39. Y. Allain, B. Bouchard, P. Imbert, and M. Perrin, *Compt. Rend.* **B263**, 9 (1966).
40. E. F. Bertaut, J. Chappert, A. Apostolov, and E. Semenov, *Bull. Soc. Franc. Miner. Crist.* **89**, 206 (1966).
41. C. Fouassier and P. Hagenmuller, *Bull. Soc. Chim. France.* 1340 (1968).
42. W. G. Mumme and J. A. Watts, *J. Solid State Chem.*, to be published.